Three-dimensional Hénon–like maps and wild Lorenz–like attractors.

S.V. Gonchenko[1], I.I. Ovsyannikov[2], C. Simó[3], D. Turaev[4]

[1]Inst. of Appl. Math. and Cyb., Nizhny Novgorod State Univ., 10 Uljanova st., Nizhny Novgorod, 603005, Russia.
[2]Radio and Physical Dept., Nizhny Novgorod State Univ., 23 Gagarina av., Nizhny Novgorod, 603000, Russia.
[3]Departament Matemàtica Aplicada i Anàlisi, Universitat de Barcelona, Gran Via, 585, 08007 Barcelona, Spain.
[4]Department of Math., Ben Gurion University, Beer Sheva 84105, Israel.

E-mail: gosv100@uic.nnov.ru, ovii@mail.ru, carles@maia.ub.es, turaev@math.bgu.ac.il

Abstract

We discuss a rather new phenomenon in chaotic dynamics connected with the fact that some three–dimensional diffeomorphisms can possess wild Lorenz–type strange attractors. These attractors persist for open domains in the parameter space. In particular, we report on the existence of such domains for a three-dimensional Hénon map (a simple quadratic map with a constant Jacobian which occurs in a natural way in unfoldings of several types of homoclinic bifurcations). Among other observations, we have evidence that there are different types of Lorenz–like attractors domains in the parameter space of the 3D Hénon map. In all cases the maximal Lyapunov exponent, Λ_1, is positive. Concerning next Lyapunov exponent, Λ_2, there are open domains where it is definitely positive, other where it is definitely negative and, finally, domains where it cannot be distinguished numerically from zero (i.e.,$|\Lambda_2| < \rho$, where ρ is some tolerance ranging between 10^{-5} and 10^{-6}). Furthermore, several other kinds of interesting attractors have been found in this family of 3D Hénon maps.

Short title: 3D Hénon maps and Lorenz attractors.

Introduction

Lorenz attractor plays a very special role in dynamical systems. The reason is that it is a genuine strange attractor, while most of the other attractors seen in various models with chaotic behavior are not. Indeed, it is well–known that even though the observed trajectory behavior may look quite chaotic for some parameter values, it happens very often that small changes in the parameters of the system change the behavior to a periodic one. One speaks about stability windows in this case, and the observed number of stability windows in the parameter space has a tendency to grow with the increase of the accuracy of measurements/simulations. It is true, however, that some of the windows can be very tiny and the total relative measure can be relatively small in some domains, but it can happen (as in the case of the logistic map) that the set of windows is dense. For given values of the parameters it can be a very difficult task to decide if the ω–limit set contains a strange attractor.

Attractors either containing stable periodic orbits of long periods, or acquiring such orbits by a small perturbation of the system, were called in Afraimovich & L.Shilnikov [1983b] quasi-attractors. It is, in fact, one of the most challenging problems in dynamics: most of the types of chaotic attractors we see in applications are definitely quasi-attractors, and it is absolutely unclear in which exact sense they are chaotic, or how to define and measure the "probability" for a quasi-attractor to be chaotic.

Lorenz attractor is free of these problems. It contains no stable periodic orbits, every orbit in it has positive maximal Lyapunov exponent, and these properties are robust with respect to changes in the parameters of the system [Afraimovich *et al.*, 1977; 1983; Guckenheimer & Williams, 1979]. The reason for that is that Lorenz attractor possesses a pseudo-hyperbolic structure in terms of Turaev & L.Shilnikov [1998] which means two things:

1) there is a direction in which the flow is strongly contracting ("strongly" means that any possible contraction in transverse directions is always strictly weaker), and

2) transverse to this direction the flow expands areas.

The expansion of areas immediately implies the positiveness of the maximal Lyapunov exponent for every orbit in the attractor, so the robustness of the pseudo-hyperbolicity property ensures the robustness of the chaotic behavior of orbits in the Lorenz attractor (although this attractor is not structurally stable [Guckenheimer, 1976; Afraimovich *et al.*, 1983]).

The pseudo–hyperbolicity is a weaker version of uniform hyperbolicity. In fact, it occurs to be weak enough to allow pseudo-hyperbolic attractors, like the Lorenz one, to exist in simple models of natural origin (contrary to hyperbolic attractors which, so far, have been relevant for specially prepared examples only). One of the reasons why Lorenz–like attractors are guaranteed to be present in models from natural applications is that systems which are known to possess the Lorenz attractor (Lorenz model [Lorenz, 1963], Shimizu–Morioka model [Shimizu & Morioka, 1980]) occur to be asymptotic normal forms for bifurcations of equilibrium states of a certain class [A.Shilnikov *et al.*, 1993; Pisarevsky *et al.*, 1998]. Namely, let a stable equilibrium loose its stability in such a way that three of its characteristic exponents vanish simultaneously. The fact that the triple instability of equilibria can lead to chaos is known since Arneodo *et al.* [1985a; b]. According to A.Shilnikov *et al.* [1993], in presence of certain discrete symmetries the behavior of the system passing through the triple instability is, looking at the dominant terms, described by one of the two models mentioned above. This implies that a small Lorenz attractor is indeed born when such equilibrium bifurcates.

It was also shown in A.Shilnikov *et al.* [1993] that a similar phenomenon happens at certain bifurcations of periodic orbits. Namely, an asymptotic normal form for the bifurcations of a periodic orbit having the triplet of multipliers $(-1,-1,1)$ is, under some conditions, the Shimizu–Morioka model with an exponentially small periodic forcing. Therefore, such bifurcation can also produce Lorenz–like attractors. Moreover, the presence of forcing (whose amplitude grows as we move away from the bifurcation point) changes the nature of the attractor. While it keeps a pseudo–hyperbolicity property, hence being a real strange attractor (see more explanations below), it no longer contains equilibrium states, contrary to the original Lorenz attractor.

Clearly, we have the same picture when we consider bifurcations of periodic orbits in discrete dynamical systems: in maps of dimension three (and more), bifurcations of periodic points with multipliers $(-1,-1,1)$ can lead to Lorenz–like attractors. In this paper we investigate this effect on the example of the following quadratic map:

$$H_{B,M_1,M_2}: \ (x,y,z) \mapsto (\bar{x},\bar{y},\bar{z}), \qquad \bar{x}=y, \ \ \bar{y}=z, \ \ \bar{z}=M_1+Bx+M_2y-z^2, \tag{1}$$

where $(x,y,z)\in\mathbb{R}^3$ and $(M_1,M_2,B)\in\mathbb{R}^3$ are parameters. It is one of the possible generalizations of the famous two–dimensional Hénon map: map (1) is quadratic and it has constant Jacobian $J\equiv B$. Therefore, we can call it the "3D Hénon map".

A numerically obtained 3D picture of iterations of a single point by (1) for $M_1=0, M_2=0.85, B=0.7$ is shown in Fig.1 left. The resemblance to the traditional picture of the Lorenz attractor is astonishing. Recall that this is a discrete trajectory of just one point. Still it mimics very well a motion along a continuous trajectory of the classical Lorenz attractor. In the figure the projection on the x,y variables is also shown, as well as "slices" of the attractor to grasp its shape. The slices have half width 10^{-5} around planes with values of z from -0.1 to 0.8 with step 0.1. The right part contains a similar picture for $M_1=0, M_2=0.815, B=0.7$, where one can better observe the role of the unstable manifold of the fixed point. Note that the attractor in the latter figure is very similar to the Lorenz attractor with a lacuna from Shimizu-Morioka system [A.Shilnikov, 1986; 1993].

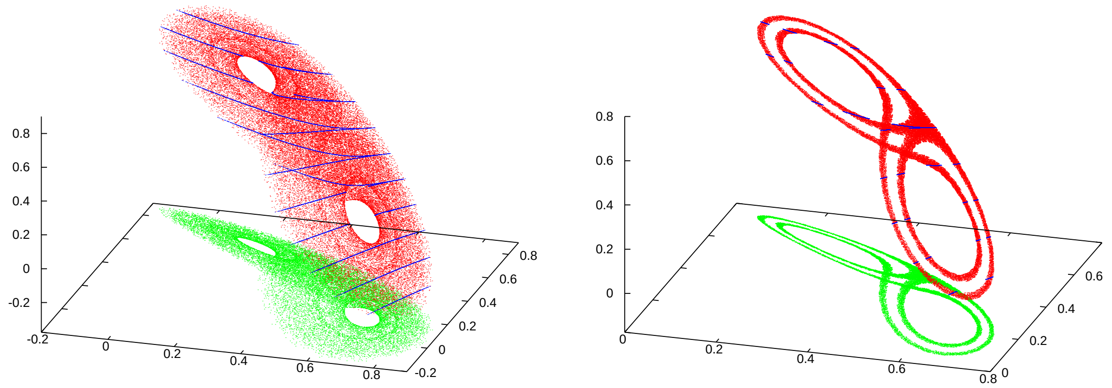

Figure 1: Plots of attractors observed numerically for $M_1=0, B=0.7$ and $M_2=0.85$ (left) or $M_2=0.815$ (right). The projections on the (x,y) variables (in green) and slices near planes of constant z (in blue) are also displayed.

In fact, there is an interesting quantitative aspect in the similarity between the behavior of discrete trajectories of map (1) and continuous trajectories of the Lorenz attractor. Indeed, we observe that the numerically computed spectrum of Lyapunov exponents of the Lorenz–like attractors of the 3D Hénon map under consideration, beyond a maximal exponent Λ_1 which is positive, contains a second exponent, Λ_2, which is close to zero, as one can expect because the orbits of the map follow orbits of a continuous flow. This exponent seems to be definitely positive, say 10^{-3}, or definitely negative, say -10^{-3}, for open sets of parameter values, while in other open sets (the red regions in Figs.5,6) it cannot be distinguished numerically from zero (the observed value of Λ_2 oscillates near zero within the range, say, 10^{-6}, and its sign does not stabilize with the increase of the length of the trajectory). However, the attractors observed for nearby values of the parameters look visually quite similar, independently of the sign of Λ_2. A standing problem is to clarify the source of these small differences in values and sign of Λ_2 and the details of the geometry of the attractors which give rise to them. More discussion see in Sec.2.1.

We remark that domains in the parameter space where two Lyapunov exponents are definitely positive (like in the present blue regions) occur in a quite different context: perturbations of a 2D Hénon map driven by the Arnold map of the circle, for values of the parameters of the latter map corresponding to quasi-periodic dynamics, see Broer *et al.* [2005]. While in the skew-product case (the 2D Hénon map driven by Arnold map) the dominant Lyapunov exponent is positive and second one is obviously zero, in the fully coupled case the second Lyapunov exponent can be either definitively positive or negative (in domains of the parameter space which do not seem to mix) despite it remains close to zero. This is in striking contrast with the behavior of present 3D Hénon model.

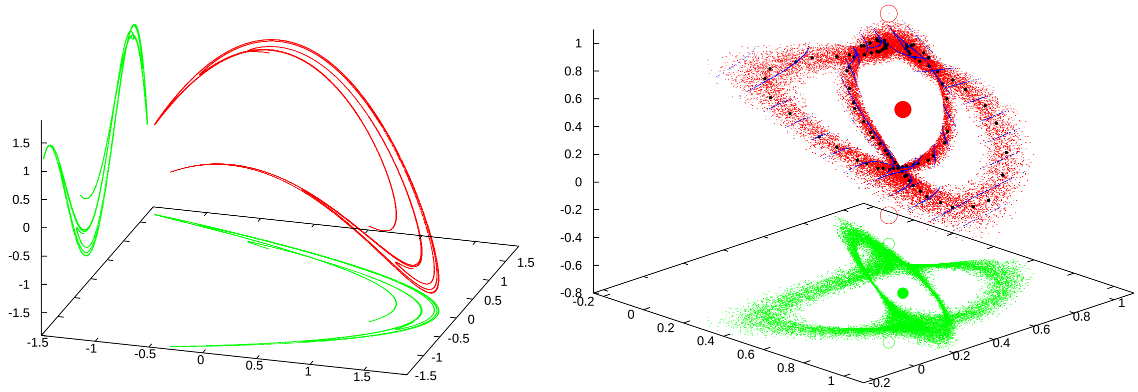

Figure 2: Left: An attractor similar to attractors found for the 2D Hénon map for $M_1 = 1.4, M_2 = 0.2, B = 0.1$. The projections on the (x, y) and on the (x, z) variables are also shown. Right: An attractor for $M_1 = 1.77, M_2 = -0.925, B = -0.95$ is displayed, as well as the projection on the (x, y) plane. Fixed point P_1 and periodic points Q_1, Q_2 are also shown, together with their projections. Slices (in blue) give an idea of the shape. Furthermore 100 iterates of some initial point under H^4_{B,M_1,M_2} are shown in black. See Sec.3 for more information on this attractor.

The importance of the 3D Hénon map goes beyond the circle of problems related to Lorenz attractors. First of all, at $B = 0$, this map has an invariant two–dimensional surface $z = M_1 + M_2 x - y^2$ (every point jumps into this surface after just one iteration for $B = 0$). On this surface the map is indeed the two–dimensional Hénon map with Jacobian $-M_2$. When $M_2 \neq 0$, every compact piece of this surface is strongly exponentially attracting (normally hyperbolic in terms of Fenichel [1971]) for all sufficiently small B. The normal hyperbolicity implies that map (1) continues to have a two-dimensional attracting invariant manifold for small B, and the dynamics on it is quite close to the one seen in the 2D Hénon map (see Fig.2 left). As B grows, this picture is destroyed, so our 3D Hénon map can serve as a paradigm for the study of the unfolding of two-dimensional maps to maps of higher dimension. On the right part of Fig.2 an attractor for $B = -0.95$ is displayed. See Sec.1 for information about fixed and periodic points and Sec.3 for further comments on that kind of attractors.

Another important issue is that the 3D Hénon map is the limit of a rescaled first return map near a homoclinic tangency to a saddle-focus periodic orbit in the case of codimension 2, which corresponds to the boundary between volume–contracting and volume–expanding maps [Gonchenko & I.I.Ovsyannikov, 2005]. It means that every dynamical phenomenon typical for the 3D Hénon map can be encountered at the bifurcations of any such tangency. Hence, everything we can learn about the dynamics of the 3D Hénon map is relevant for the general problem of the behavior of attractors of three–dimensional non–hyperbolic maps without the volume–contracting property.

One more possible 3D generalization of the 2D Hénon map is written as

$$(x, y, z) \mapsto (\bar{x}, \bar{y}, \bar{z}), \qquad \bar{z} = y, \bar{y} = x, \ , \ \bar{x} = M_1 + M_2 x + Bz + By^2. \tag{2}$$

This map is the inverse of the map $H_{B^{-1},-BM_1,-BM_2}$ (see (1)), so its attractors are repellers of map (1), and, as a preliminary study shows, they are quite different from the attractors of map (1). Map (2), although not considered in the present paper, is equally interesting for the theory of homoclinic bifurcations, as it is also a limit of a rescaled first return map near certain homoclinic tangencies [Gonchenko *et al.*, 1993; 2003]. We plan to consider map (2) in a forthcoming paper.

In Sec.1 we present some key points of the dynamics of the family (1). Then, in Sec.2, flows which approximate the family of diffeomorphisms for suitable values of the parameters, are constructed and the arguments to prove the existence of Lorenz–like attractors are given. Finally, Sec.3 is devoted to illustrate, by a numerical study, that the predicted behavior is indeed found in the family (1), it has a rather large range of validity and several other interesting phenomena are also found on it.

1 Some elements of the dynamics of the 3D Hénon map

Map (1) has, at most, two fixed points, their coordinates being given by

$$x = y = z = x^*, \qquad x^* = \frac{B + M_2 - 1}{2} \pm \sqrt{\frac{(B + M_2 - 1)^2}{4} + M_1}. \tag{3}$$

These points are born at a saddle–node bifurcation (that corresponds to a multiplier equal to 1) on the surface

$$L^+ \ : \ M_1 = -\frac{(M_2 + B - 1)^2}{4}$$

in the parameter space. We denote the fixed points as P_1 and P_2, where P_1 corresponds to the sign "+" in (3), and P_2 to the sign "−".

The surface

$$L_1^- \ : \ M_1 = \frac{1 - M_2 + B}{4}(3 - 3M_2 - B), \ \ M_2 \leq 1$$

corresponds to the period–doubling bifurcation (a multiplier equal to −1) of the fixed point P_1; the surface

$$L_2^- \ : \ M_1 = \frac{1 - M_2 + B}{4}(3 - 3M_2 - B), \ \ M_2 \geq 1$$

corresponds to the period-doubling of P_2. Transition across the surface L_1^- or L_2^- leads to the birth of a period two orbit (Q_1, Q_2) where $Q_1 = (t_1, t_2, t_1)$ and $Q_2 = (t_2, t_1, t_2)$,

$$t_{1,2} = \frac{B - M_2 + 1}{2} \pm \sqrt{\frac{(B - M_2 + 1)(B - 3 + 3M_2)}{4} + M_1}.$$

This is the only period two orbit of map (1), its domain of existence being the region

$$M_1 > \frac{1 - M_2 + B}{4}(3 - 3M_2 - B).$$

The surface

$$L^\varphi \;:\; M_1 = (1 - B)^2 \left(1 + \frac{M_2 + 1}{2B}\right)^2 - \frac{(B + M_2 - 1)^2}{4}, \quad |M_2 + 1| < 2|B|,$$

corresponds to the case where the fixed point P_1 (when $B \le 1$), or the fixed point P_2 (when $B \ge 1$) has a pair of multipliers $e^{\pm i\varphi}$, $0 < \varphi < \pi$ with $2\cos\varphi = -(M_2 + 1)/B$. This bifurcation is responsible for the birth of an invariant curve from the corresponding fixed point. One can check that both subcritical and supercritical bifurcations are possible here. The supercritical bifurcation of a stable fixed point leads to the birth of an attracting invariant curve. In fact, zones with attracting invariant curves are present in abundance in the parameter space. One can observe resonant phenomena and, in the spirit of Afraimovich & L.Shilnikov [1974; 1983a], Broer *et al.* [1998], A.Shilnikov *et al.* [2004], the breakdown of invariant curves, with the further transition to chaos (see Fig.4 in Sec.3 and the corresponding discussion).

It is not hard to see that the fixed point P_2 is never stable, while the stability region of the fixed point P_1 is the region bounded by the surfaces L^+, L_1^-, L^φ and $|B| = 1$. Namely, for each $B^* \in (-1, 1)$, the intersection of the stability region of P_1 with the plane $B = B^*$ is a curvilinear triangle bounded by the curve $L^\varphi \cap \{B = B^*\}$, the arc of the curve $L^+ \cap \{B = B^*\}$ between $M_2 = -2B^* - 1$ and $M_2 = 1$ (at $M_2 = -2B - 1$ the surface L^φ adjoins L^+, and at $M_2 = 1$ the surface L_1^- adjoins L^+), and the arc of the curve $L_1^- \cap \{B = B^*\}$ between $M_2 = +2B^* - 1$ and $M_2 = 1$ (at $M_2 = 2B - 1$ the surface L^φ adjoins L^-). As an example, see the bifurcation diagrams on the plane (M_1, M_2) for different values of B in Fig.3.

When leaving the stability region across the surface L_1^-, the point P_1 becomes a saddle with a one-dimensional unstable manifold which is divided by P_1 into two components, the separatrices (each separatrix is the image of the other one by the map). The separatrices tend to the points Q_1 and Q_2 of the newly born stable orbit of period two. This orbit can also undergo bifurcations: it has a pair of multipliers $e^{\pm i\varphi}$ on the unit circle at

$$\begin{aligned} M_1 &= -\frac{1}{2}\cos\varphi + \frac{M_2}{2} - \frac{B^2}{4} + (1 - M_2 + B)(1 - M_2), \\ \cos\varphi &= 1 + \frac{(1 - M_2)(2B - M_2 - 1)}{2B^2}, \end{aligned}$$

and it has a multiplier equal to (-1) at

$$M_1 = \frac{3}{4}(B + 1 - M_2)^2 + \frac{1 + M_2^2}{2}.$$

Even prior to these bifurcations, the separatrices of the fixed point can detach from the period two orbit. As we show in the next Section, a Lorenz–like strange attractor that contains the saddle fixed point P_1 and its separatrices can be formed in this way.

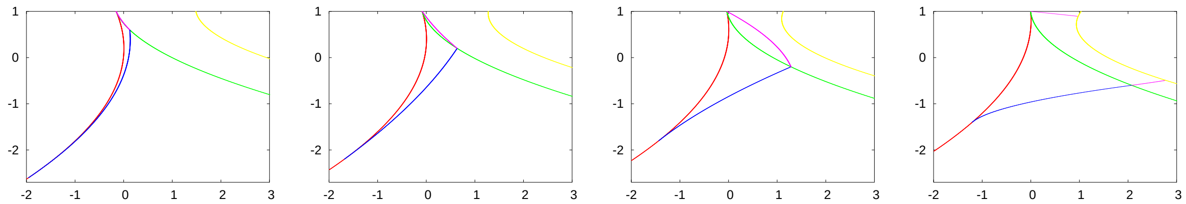

Figure 3: Bifurcation diagrams on the (M_1, M_2) plane for $B = 0.8, 0.6, 0.4, 0.2$ (from left to right). The color codes for the curves are: L^+: red; L_1^-: green; L^φ: blue; multipliers on the unit circle of period two orbit: magenta; multiplier (-1) for the period two orbit: yellow.

2 The birth of a small Lorenz–like attractor from a fixed point of the 3D Hénon map

We will now prove that a small Lorenz–like attractor indeed exists at parameter values near $(M_1 = -1/4, M_2 = 1, B = 1)$. At these exact values, the fixed point of the map has the following triplet of multipliers: $(1, -1, -1)$. As we mentioned, it was shown in A.Shilnikov *et al.* [1993] that bifurcation of points with such multipliers can lead to the birth of a Lorenz–like attractor under certain conditions. We shall show now that these conditions are indeed fulfilled by the 3D Hénon map under consideration.

Since we are interested in attractors, we will focus on the behavior in the parameter region which adjoins the point $(M_1 = -1/4, M_2 = 1, B = 1)$ from the side $B < 1$. This guarantees the contraction of volumes which is a necessary condition for a map with a constant Jacobian to have attractors. We also restrict our attention to the analysis of the behavior in a small neighborhood of the fixed point P_1.

Shifting the coordinates $x \to x - x^*, y \to y - x^*, z \to z - x^*$ where x^* was given in (3) brings the point P_1 into the origin. The map (1) takes the form

$$\bar{x} = y, \quad \bar{y} = z, \quad \bar{z} = Bx + M_2 y - 2x^* z - z^2 \,. \tag{4}$$

We introduce new parameters $\varepsilon_1, \varepsilon_2, \varepsilon_3$:

$$\varepsilon_1 = 1 - B, \quad \varepsilon_2 = 1 - M_2, \quad \varepsilon_3 = 2x^* - 1.$$

Using $B < 1$ and (3) we obtain

$$\varepsilon_1 > 0, \quad \varepsilon_1 + \varepsilon_2 + \varepsilon_3 > 0.$$

Note also the following relation

$$4M_1 = (\varepsilon_1 + \varepsilon_2 + \varepsilon_3)^2 - (\varepsilon_1 + \varepsilon_2 - 1)^2$$

between the new parameters and M_1.

Let γ be the multiplier of the zero fixed point of map (4) which is close to 1:

$$\gamma = 1 - \frac{\varepsilon_1 + \varepsilon_2 + \varepsilon_3}{4} + O(\|\varepsilon\|^2).$$

Let us make the following linear coordinate transformation:

$$v_1 = -\gamma x + y, \quad v_2 = \gamma x + (\gamma - 1)y - z, \quad v_3 = \gamma(1 - \varepsilon_1)x + (1 - \varepsilon_1 + \gamma(1 - \varepsilon_2))y + \gamma^2 z.$$

Map (4) takes the following form

$$\begin{aligned}
\bar v_1 &= -v_1 - v_2,\\
\bar v_2 &= -\alpha_1 v_1 + (-1+\alpha_2)v_2 + \frac{(2v_1+3v_2-v_3)^2}{16} + O(\|v\|^3 + \|v\|^2\|\varepsilon\|),\\
\bar v_3 &= (1-\alpha_3)v_3 - \frac{(2v_1+3v_2-v_3)^2}{16} + O(\|v\|^3 + \|v\|^2\|\varepsilon\|),
\end{aligned} \tag{5}$$

where

$$\begin{aligned}
\alpha_1 &= \gamma + \varepsilon_3 - \frac{1-\varepsilon_1}{\gamma} = \frac{\varepsilon_1 - \varepsilon_2 + \varepsilon_3}{2} + O(\|\varepsilon\|^2),\\
\alpha_2 &= 1 - \gamma - \varepsilon_3 = \frac{\varepsilon_1 + \varepsilon_2 - 3\varepsilon_3}{4} + O(\|\varepsilon\|^2),\\
\alpha_3 &= 1 - \gamma = \frac{\varepsilon_1 + \varepsilon_2 + \varepsilon_3}{4} + O(\|\varepsilon\|^2).
\end{aligned}$$

Note that the linear part of (6) is in Jordan form at $\varepsilon = 0$.

Some quadratic terms can be cancelled by an additional normalising transformation:

$$\begin{aligned}
u_1 &= v_1 + (4v_1^2 + 4v_1v_2 - v_2^2 + v_3^2)/64,\\
u_2 &= v_2 - (4\bar v_1^2 + 4\bar v_1\bar v_2 - \bar v_2^2 + \bar v_3^2)/64 - (4v_1^2 + 4v_1v_2 - v_2^2 + v_3^2)/64,\\
v_3 &= v_3 + v_3(v_2 + v_1)/8.
\end{aligned}$$

The map takes then the form

$$\begin{aligned}
\bar u_1 &= -u_1 - u_2,\\
\bar u_2 &= -\alpha_1 u_1 + (-1+\alpha_2)u_2 - \frac{(2u_1+3u_2)u_3}{8} + O(\|u\|^2\|\varepsilon\| + \|u\|^3),\\
\bar u_3 &= (1-\alpha_3)u_3 - \frac{(2u_1+3u_2)^2 + u_3^2}{16} + O(\|u\|^2\|\varepsilon\| + \|u\|^3),
\end{aligned} \tag{6}$$

One checks that the composition of map (6) with the involution

$$\sigma:\ (u_1, u_2, u_3) \leftrightarrow (-u_1, -u_2, u_3) \tag{7}$$

gives a map whose linear part at the origin has Jordan form $\begin{pmatrix} 1 & 1 & 0\\ 0 & 1 & 0\\ 0 & 0 & 1\end{pmatrix}$ at $\varepsilon = 0$ and coincides, up to terms of order $O(\|u\|^2\|\varepsilon\| + \|u\|^3)$, with the time 1 shift by the flow

$$\begin{aligned}
\dot u_1 &= \hat\beta_1 u_1 + (1+\hat\beta_2)u_2 - \frac{1}{8}u_1u_3 - \frac{5}{48}u_2u_3,\\
\dot u_2 &= \beta_1 u_1 - \beta_2 u_2 + \frac{1}{4}u_1u_3 + \frac{1}{4}u_2u_3,\\
\dot u_3 &= -\beta_3 u_3 - \frac{1}{4}u_1^2 - \frac{1}{2}u_1u_2 - \frac{11}{48}u_2^2 - \frac{1}{16}u_3^2.
\end{aligned} \tag{8}$$

where

$$\begin{aligned}
\beta_3 &= -\ln(1-\alpha_3) = \frac{\varepsilon_1+\varepsilon_2+\varepsilon_3}{4} + O(\|\varepsilon\|^2),\\
&\begin{pmatrix} \hat\beta_1 & 1+\hat\beta_2\\ \beta_1 & -\beta_2\end{pmatrix} = \ln\begin{pmatrix} 1 & 1\\ \alpha_1 & 1-\alpha_2\end{pmatrix}.
\end{aligned}$$

The latter implies

$$\begin{aligned}
\hat\beta_1 &= -\frac{\varepsilon_1 - \varepsilon_2 + \varepsilon_3}{4} + O(\|\varepsilon\|^2), \quad \hat\beta_2 = \frac{7\varepsilon_1 - \varepsilon_2 - 5\varepsilon_3}{24} + O(\|\varepsilon\|^2),\\
\beta_1 &= \frac{\varepsilon_1 - \varepsilon_2 + \varepsilon_3}{2} + O(\|\varepsilon\|^2), \quad \beta_2 = \frac{\varepsilon_1 - \varepsilon_3}{2} + O(\|\varepsilon\|^2).
\end{aligned}$$

Let us now scale the coordinates (u_1, u_2, u_3), the time t, and the parameters as follows:

$$t = \tau/s, \quad u_1 = 4s^{3/2}X, \quad u_2 = 4s^{5/2}Y, \quad u_3 = -4s^2 Z, \quad \beta_2 = s\lambda, \quad \beta_3 = s\alpha, \tag{9}$$

where the small scaling factor s is

$$s = \sqrt{\beta_1}. \tag{10}$$

We are interested in values of (α, λ) in a bounded domain of the positive quadrant. This implies that we consider our system in the region of parameters ε where the value β_1 is positive and of the order $O(\|\beta_2\|^2 + \|\beta_3\|^2)$. Since s becomes arbitrarily small as we approach the bifurcation point $\varepsilon = 0$ in the initial parameter space, it follows that the rescaled coordinates (X, Y, Z) and new parameters λ and α can take arbitrarily finite values.

After the scaling, the system (8) becomes $O(s)$-close to the Shimizu-Morioka system

$$\begin{aligned} \dot{X} &= Y, \\ \dot{Y} &= X(1 - Z) - \lambda Y, \\ \dot{Z} &= -\alpha Z + X^2, \end{aligned} \tag{11}$$

where the dot denotes $d/d\tau$. An extensive analysis of this model was undertaken in A.Shilnikov [1986; 1993]. It was shown there that the system has a Lorenz attractor for a certain open domain of positive values of the parameters α and λ. See Fig.4 in Sec.3 for illustrations on that domain and other properties of the Shimizu-Morioka system. The existence of a Lorenz attractor is a robust property [Afraimovich *et al.* 1983], i.e. every system close enough to (11) has to have a Lorenz attractor in a nearby region of the (α, λ)-values. Since, as we have shown, the flow map of (11) is a close approximation of map (1) near the bifurcation point, the existence of a Lorenz–like attractor for the the 3D Hénon map will follow.

Indeed, since the fixed point at zero of map (6) has multipliers $(-1, -1, 1)$ at $\varepsilon = 0$, the standard normal form theory (for details see, for example, L.Shilnikov *et al.* [1998]) gives us that in appropriately chosen coordinates the composition of the map with the involution (7) can be approximated up to terms of any arbitrarily high order by the time 1 map of an autonomous flow which commutes with the above involution. In other words, one can choose new coordinates $w = (w_1, w_2, w_3)$, obtained from (u_1, u_2, u_3) by a close to the identity transformation, C, in such a way that the map (6) will coincide with the composition of the involution (7) and the time 1 map of a flow

$$\dot{w} = W_1(w) + W_2(w) + W_3(w, t), \tag{12}$$

where $W_1(w)$ is the right-hand side of (8), $W_2(w) = O(\|w\|^2\|\varepsilon\| + \|w\|^3)$ is a function of w and ε such that $W_2(\sigma w) = \sigma W_2(w)$, where σ denotes the involution (7) and $W_3(w, t)$ is 1-periodic in t. Furthermore, for any arbitrarily large N, one can choose a transformation $C = C_N$ such that $\|W_3\| = o(\|w, \varepsilon\|^N)$ for w in a fixed compact and all t.

If the initial diffeomorphism is analytic (as it happens in our case) and we recall that the original time has been scaled by the small parameter s, then the transformation C can be chosen to be analytic in (w, ε) on a fixed compact and the vector fields $W_j, j = 1, 2, 3$ are also analytic in (w, ε) on a compact. Furthermore, the bound $\|W_3\| < \exp(-c/s)$ holds for some $c > 0$. This follows from averaging theory as in Neishtadt [1984]. See, e.g., Broer *et al.* [1996] for details in a similar case.

After the rescaling (9),(10) system (12) takes the form

$$\frac{d}{d\tau}\begin{pmatrix} X \\ Y \\ Z \end{pmatrix} = V_1(X, Y, Z, \alpha, \lambda) + V_2(X, Y, Z, \alpha, \lambda) + V_3(X, Y, Z, \alpha, \lambda, \tau/s) \tag{13}$$

where $V_2 = O(s)$ is independent of τ and it is symmetric with respect to the involution $\bar{\sigma}$: $(X, Y, Z) \leftrightarrow (-X, -Y, Z)$, the non-autonomous part is exponentially small in s, and V_1 is the right-hand side of the Shimizu-Morioka system (11).

The existence of the Lorenz attractor in the Shimizu-Morioka system implies that, for all s sufficiently small, the time-independent part $\bar{V}$ of system (13):

$$\frac{d}{d\tau}\begin{pmatrix} X \\ Y \\ Z \end{pmatrix} = V_1(X, Y, Z, \alpha, \lambda) + V_2(X, Y, Z, \alpha, \lambda) =: \bar{V}, \tag{14}$$

has a Lorenz attractor in an appropriate region of (α, λ).

Furthermore, the time s map has also a strange attractor which is a discrete version of the attractor found for $\bar{V}$. The difference between the time s map of $\bar{V}$ and the composition of the involution σ with the 3D Hénon map (in w variables) is only due to the contribution of the non-autonomous term V_3 in (13). Because of the smallness of V_3 we can, finally, conclude that in an appropriate region of parameters adjoining the bifurcation point $(M_1 = -1/4, M_2 = 1, B = 1)$ (that corresponds to $\varepsilon = 0$) the orbits of the map (1) near the fixed point P_1 follow very closely and for a long time orbits in the Lorenz attractor of system (14) (while the even iterations follow a certain orbit of (14), the odd iterations follow the image of this orbit under the symmetry $\bar{\sigma}$). This explains the striking similarity of the numerically obtained pictures of iterations of map (1) with the well-known pictures of the Lorenz model, which are also found in the Shimizu-Morioka system.

2.1 On the wild character of the attractors

In fact, there is more than simply a similarity of the pictures here. Based on the theory developed in Turaev & L.Shilnikov [1998; 2005] one can show that the Lorenz–like attractor we obtain at sufficiently small ε is indeed a strange attractor, and we can also describe its nontrivial properties. As we mentioned, when speaking about a classical Lorenz attractor we mean that the system under consideration has an absorbing domain where the flow has a pseudo-hyperbolic structure: it has a strongly-stable invariant foliation of codimension two and it uniformly expands area in the directions transverse to the foliation. Moreover, one assumes that there is a saddle equilibrium in the absorbing domain and that all orbits, except for the equilibrium, intersect a certain cross–section. Based on this one can prove that the system has a unique attractor, which is defined [Turaev & L.Shilnikov, 1998] as the only Lyapunov stable chain-recurrent set (for a more traditional view on the Lorenz attractor see Afraimovich et al. [1993]), and the attractor is strange in the sense that every orbit in it has a positive maximal Lyapunov exponent. It is obvious that applying a small periodic forcing to such system (this is the situation at which we arrive when analysing the bifurcations of the fixed point with the multipliers $(-1, -1, 1)$ in map (1), see (13)) does not destroy the strongly stable invariant foliation while the property of the transverse area expansion transforms to the uniform expansion of volumes in the directions transverse to the foliation (adding the periodic forcing increases the dimension of the phase space by adding a cyclic time variable; in this direction the flow is neither contracting, nor expanding, so the area-expanding flow becomes volume-expanding). The expansion of transverse volumes implies the existence of a positive maximal Lyapunov exponent for every orbit immediately (there is a similar result in Sataev [in preparation]). More to that, one can show [Turaev & L.Shilnikov, 2005] that if the forcing is small, the system still has a unique stable chain-recurrent invariant set (the attractor) and that this attractor is wild in the sense that it contains a Newhouse wild hyperbolic set for an open set of parameter values, and it contains arbitrarily degenerate periodic and homoclinic orbits for a dense set of parameter values. Thus, although the attractor we see in map (1) looks very much Lorenz–like, subtle details of the orbit behavior are here much more complicated than for the standard Lorenz attractors.

It is known [Afraimovich *et al.*, 1983] that saddle periodic orbits are dense within the transitive component of the Lorenz attractor. When a small s-periodic forcing is applied, the periodic orbits are transformed into saddle invariant tori (closed invariant curves for the time-s map). The tori should no longer form a dense set. Nevertheless, according to L.Shilnikov [1969], Afraimovich & L.Shilnikov [1982], there is an infinite set of them coded by arbitrary sequences of two symbols. Such sets of tori exist for open regions in the parameter space of systems with a periodically perturbed Lorenz attractor, hence in the parameter space of the 3D Hénon map. One can deduce from Gorodetskij & Ilyashenko [1999; 2000], that in the closure of such set of invariant circles there exists at least one orbit of our map with one zero Lyapunov exponent (moreover, there exists an ergodic invariant measure with a zero Lyapunov exponent [Gorodetskij *et al.*, 2005]), and this property holds true for an open set of parameter values. Surprisingly, as we see in Figs.5,6, this "non-hyperbolicity" property is quite visible: for all tested values from the red regions in these Figures, a numerically computed spectrum of Lyapunov exponents of a randomly chosen orbit of the 3D Hénon map includes a quite close to zero exponent indeed. Whether this numerical effect is really related to the above mentioned results of Gorodetskij *et al.* [1999; 2000; 2005], or it is a manifestation of exponential smallness of the effective forcing, this is not clear so far.

3 Numerical observation of Lorenz–type attractors in the 3D Hénon maps

Before presenting the results of some numerical experiments for the 3D Hénon map we shall display some results for the Shimizu-Morioka system (11). A detailed exposition of the plethora of bifurcational phenomena in that system can be found in A.Shilnikov [1986; 1993]. Based on numerical evidence and the theory of Afraimovich *et al.* [1993], it was concluded in A.Shilnikov [1986; 1993] that Lorenz–like attractors exist in the Shimizu-Morioka system in a persistent way, i.e., for open domains in (α, λ). For concrete values of the parameters a computer assisted proof, like the one given in Tucker [1999] for Lorenz system, has to be performed. Alternatively, one may try to prove formally the existence of Lorenz attractor domains in the parameter space of the Shimizu-Morioka system with the use of the criteria from L.Shilnikov [1981] and the technique of proving the existence of homoclinic loops due to Belykh [1984], or Robinson [1989; 1992], or Rychlic [1990], see more discussion in A.Shilnikov *et al.* [1993].

The numerical tool we have used is the computation of the Lyapunov exponents, scanning for the (α, λ) parameters. It is clearly enough to compute the two dominant ones $\Lambda_1 \geq \Lambda_2$ as $\Lambda_1 + \Lambda_2 + \Lambda_3 = -\lambda$. This is easily achieved by integration of the variational equations and successive orthonormalisation. The initial point has been always taken close to the origin on the unstable manifold of the fixed point.

The results are presented in Fig.4 (left) and show several possibilities: it is attracted by one of the equilibrium states located at $(\pm\sqrt{\alpha}, 0, 1)$, by a stable periodic orbit, which can be normally of focus or node type, or by what looks like a strange attractor. Finally, it can also escape. The types of attractors are detected, from Λ_1, Λ_2 by the conditions

$$0 > \Lambda_1 \geq \Lambda_2, \quad 0 = \Lambda_1 > \Lambda_2 = \Lambda_3, \quad 0 = \Lambda_1 > \Lambda_2 > \Lambda_3 \quad \text{and} \quad \Lambda_1 > 0 = \Lambda_2,$$

respectively. Of course, these conditions are checked with some tolerance (typically between

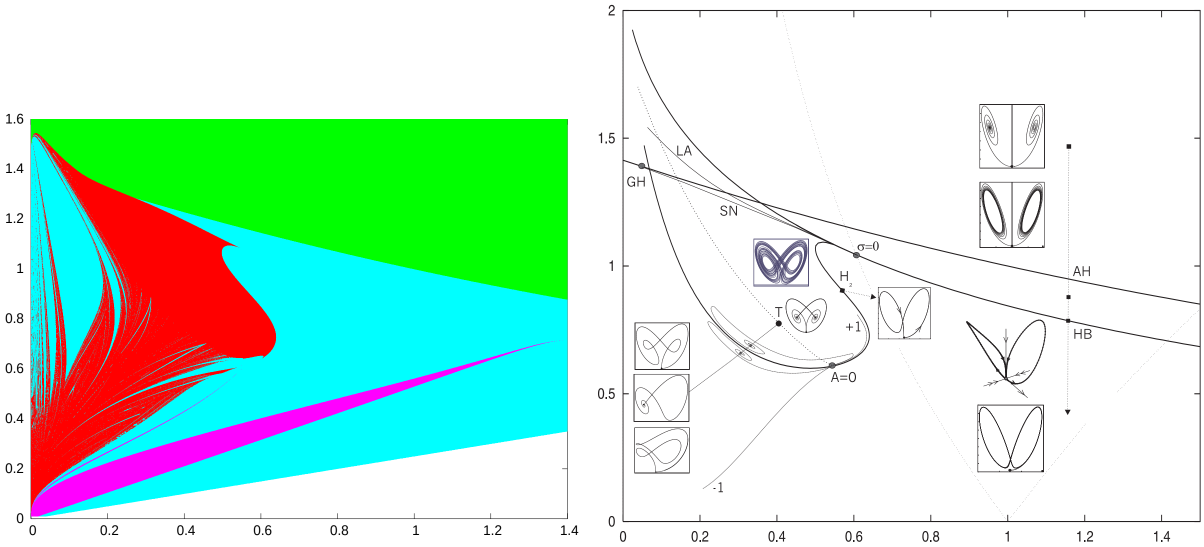

Figure 4: Left: Attractors found for the Shimizu-Morioka model starting on the unstable manifold of the origin. Colour code: green: stable equilibrium state (of focus type); light blue: stable periodic orbit with nodal normal behavior; magenta: periodic orbit with focal normal behavior; red: strange attractor. Right: The bifurcation diagram due to A.Shilnikov [1993]. The dashed line separates, with a good precision, the Lorenz attractor region from the region of a quasi-attractor. Variables plotted (α, λ).

10^{-5} and 10^{-6}, depending on the computations) and integrations are stopped as soon as an equilibrium state or a periodic orbit is approached, refining then the periodic orbit numerically. The color code associated to each domain is explained in Fig.4. The big region of persistent strange attractors is located, roughly, around $(\alpha, \lambda) = (0.4, 1)$.

This region consists visibly of two parts: in the upper and right part the behavior is chaotic for all parameter values, while in the lower left part the region is penetrated by stability windows. The divide between these two parts goes quite well along the bifurcation curve from A.Shilnikov [1986; 1993] which separates the region of existence of the Lorenz attractor from the quasi-attractor region, see Fig.4(right). Analogous bifurcation curve for the Lorenz model was built in Bykov & A.Shilnikov [1989]. The T-point on this curve is a codimension-2 point corresponding to a heteroclinic cycle involving all three equilibria (the saddle at zero and the two saddle-foci at $(\pm\sqrt{\alpha}, 0, 1)$); a bunch of similar codimension-2 points exists below the curve. According to Bykov [1980; 1993], each of the T-points on the parameter plane is a limit of an infinite series of other T-points, from each an infinite number of bifurcation curves emanates that correspond to homoclinic loops to the saddle-foci, and onto each an infinite number of bifurcation curves spiral that correspond to multiround homoclinic lops to the saddle; three of such curves are shown in Fig.4(right). Approaching the bifurcations of saddle-focus loops causes period-doubling bifurcations, so the abundance of the stability windows corresponding both to stable periodic orbits with nodal and focal behavior, see Fig.4(left), is natural. See more on the relation between saddle-focus homoclinic and heteroclinic cycles and stable periodic orbits in Afraimovich *et al* [1980], I.M.Ovsyannikov & L.Shilnikov [1987; 1991].

Above the dashed curve, as the numerical evidence of A.Shilnikov [1986; 1993] suggests, we have a genuine Lorenz attractor. The upper and right boundaries of the Lorenz attractor region (line LA in Fig.4(right), and a line, not shown, following closely line H2) correspond to the separatrices of the zero saddle equilibrium approaching certain saddle limit cycles, in agreement with the canonical scenarios from Afraimovich *et al.* [1983]: on the upper boundary a "solid" Lorenz attractor is formed, while the Lorenz attractor born on the right boundary has a "lacuna" (compare with the attractors in Fig.1). The tips of the Lorenz attractor region in Fig.4 correspond to codimension-2 homoclinic bifurcations of L.Shilnikov [1981] (see also A.Shilnikov [1986], Robinson [1989; 1992], Rychlic [1990], L.Shilnikov *et al.* [2001]): the saddle value σ vanishes on line HB of single-round homoclinic loops to the saddle, and the separatrix value A vanishes on line H2 of double-round loops. For more detail see A.Shilnikov [1986; 1993] and A.Shilnikov *et al.* [1993].

We note also that there is a domain of escape on the lower part of Fig.4 bounded exactly by the line $\lambda = \alpha/4$. This boundary corresponds to an attracting periodic orbit which escapes to infinity when $\lambda \to \alpha/4 + 0$. This can be proved by using the scalings

$$X = \bar{X}/\nu, \quad Y = \bar{Y}/\nu^2, \quad Z = \bar{Z}/\nu^2, \quad \tau = \bar{\tau}\nu$$

and letting $\nu \to 0$. The system for the rescaled variables $(\bar{X}, \bar{Y}, \bar{Z})$ as functions of $\bar{\tau}$ depends on the parameter ν and has elementary periodic solutions at $\nu = 0$. Then, standard averaging procedures allow one to compute a periodic solution at small ν, using expansion in the powers of ν by Lindstedt-Poincaré method, under the requirement $\lambda = \alpha/4 + \nu^2$. The amplitude of this solution remains finite as $\nu \to 0$. Returning to the non-rescaled variables (X, Y, Z) thus gives us a periodic solution whose amplitude tends to infinity as $\lambda \to \alpha/4 + 0$. That boundary continues up to $\alpha \simeq 1.86$ when another attracting periodic orbit shows up.

Then we passed to the 3D Hénon map. In a similar way Lyapunov exponents have been computed by iteration of the differential map and successive orthonormalisation. As before the sum of the Lyapunov exponents is known and equals $\log(|B|)$. Typically we have proceeded to scan with respect to (M_1, M_2) for several values of B. As initial points several possibilities have been used, all of them in some of the unstable manifolds of the points P_1, P_2, Q_1, in that order. It is clear that for given (B, M_1, M_2) several attractors can coexist. In that case computations have been stopped as soon as one attractor is detected. Also computations are stopped if a fixed or periodic point (of any period less than 10^6) is approached. A small sample of the results is displayed on Fig.5 for some representative values of B : 0.1, 0.5, 0.7, −0.95.

Assuming $\Lambda_1 \geq \Lambda_2 \geq \Lambda_3$ the following possibilities have been found (in cases in which some of the initial points we tried is not escaping):

1. $0 > \Lambda_1$, which corresponds to fixed or periodic attracting point, displayed in green;

2. $\Lambda_1 = 0 > \Lambda_2 = \Lambda_3$, which corresponds, as the visual inspection showed, to an invariant curve of focal normal behavior, displayed in magenta;

3. $\Lambda_1 = 0 > \Lambda_2 > \Lambda_3$, which corresponds to an invariant curve of nodal normal behavior, displayed in light blue;

4. $\Lambda_1 > 0 > \Lambda_2 > \Lambda_3$, which corresponds to a strange attractor, typically looking Hénon–like, displayed in yellow;

5. $\Lambda_1 > 0 = \Lambda_2 > \Lambda_3$, which corresponds to a strange attractor, typically looking Lorenz–like, displayed in red;

6. $\Lambda_1 > \Lambda_2 > 0 > \Lambda_3$, which corresponds to a strange attractor with two positive Lyapunov exponents, looking as a Lorenz–like attractor but perhaps "thicker", displayed in blue.

It should be kept in mind that the sign "=" means here that the difference is less than some tolerance.

It has also been checked that while in the Hénon–like attractor domains a detailed scanning (for instance, fixing B and M_1 and letting M_2 vary with step-size as small as 10^{-8} for intervals of length 0.01) shows a good abundance of "windows" of attracting periodic orbits, these windows are absent in selected domains of the Lorenz–like attractors which adjoin to the point of $(-1, -1, 1)$-bifurcation (both in the red and in a part of the blue region).

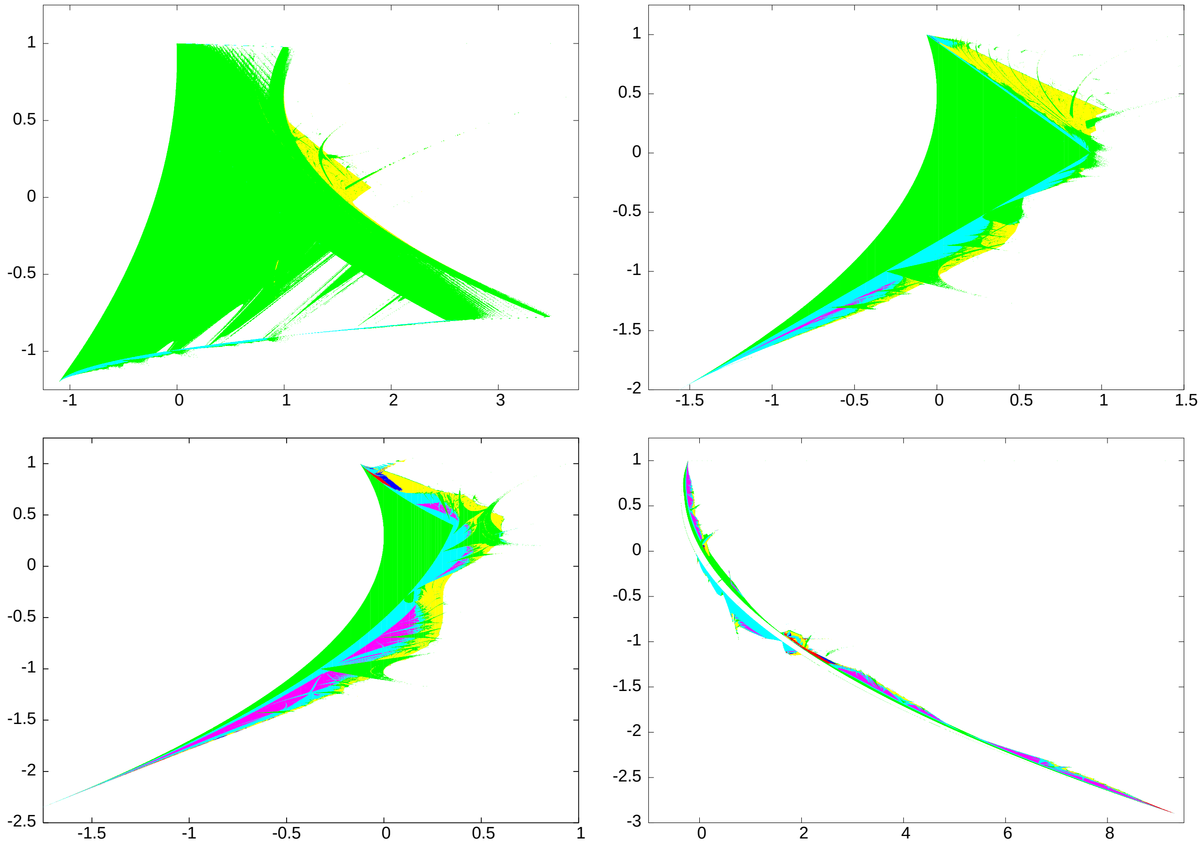

Figure 5: Attractors found for the 3D Hénon map (1) for $B = 0.1$ (top left), $B = 0.5$ (top right), $B = 0.7$ (bottom left), $B = -0.95$ (bottom right). Variables plotted $(M_1.M_2)$. See the text for color codes.

The results for small $|B|$, as expected, display mainly the 2D Hénon pattern. The strange attractors correspond to the yellow zones on the top plots in Fig.5. They are crossed by very narrow (hardly visible with the resolution of the plot, except for period 3) green strips corresponding to periodic sinks. Only the regions where two of the large strips meet (the so-called "cross-road areas", see Bosch *et al.* [1991a; b]) are well visible with the resolution of the plot. For $B = 0.5$ these strips of periodic sinks are more visible. For $B = 0.7$ Lorenz–like attractors are found not too far from the parameters predicted for $B = 1 - \varepsilon_1$. We return later to this point. Furthermore one can see zones of invariant curves which are interrupted by zones of sinks (the well-known Arnold tongues, one of the sources of destruction of smooth invariant curves, see Afraimovich & L.Shilnikov [1983a], Broer *et al.* [1998], A.Shilnikov *et al* [2004]. After these tongues Hénon–like attractors are found. For larger values of $B < 1$ the situation is similar but the regions of Lorenz–like attractors shrink (in agreement with the theory) to become almost invisible near the tip.

For $B < 0$ and moderate values, the situation is similar, concerning strange attractors, to the case of small $B > 0$. However for B approaching -1 an interesting phenomenon occurs. Beyond some extremely narrow "red" zones which appear near the tip close to $(M_1, M_2) = (-1/4, 1)$ corresponding to the $(-1, -1, -1)$-bifurcation (based on the normal form analysis from Arneodo *et al.* [1985a] one can conclude that these zones should correspond to an exponentially small perturbation of a spiral quasi-attractor), a more important region of this type appears near $(M_1, M_2) = (7/4, -1)$. This must be related to the fact that for $(B, M_1, M_2) = (-1, 7/4, -1)$ the fixed point P_1 has multipliers $-1, \pm i$. The fourth power of the map can be approximated by a flow in suitable domains. An analysis of what seems a new source of Lorenz–like attractors is planned for the future (an appropriate rescaled flow normal form should be found in Pisarevsky *et al.* [1998]). Magnifications of selected zones of Fig.5 for $B = 0.7$ and $B = 0.95$ are shown in Fig.6.

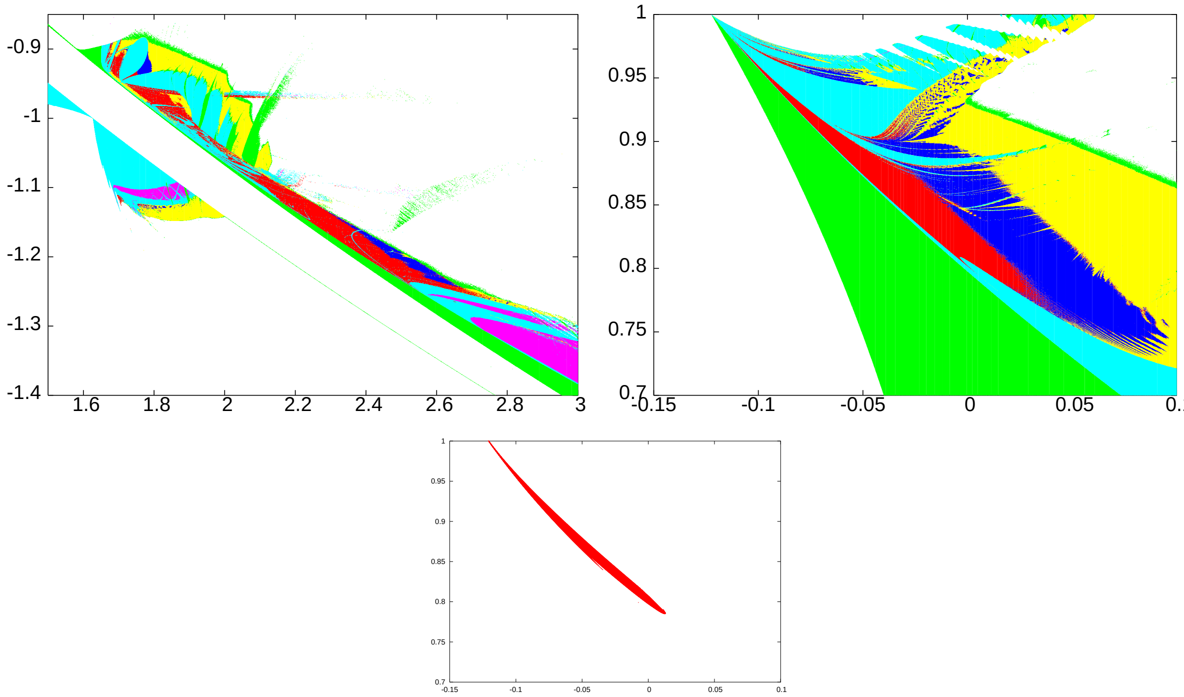

Figure 6: Magnifications of some of the plots in Fig.5 in regions where strange attractors are found. Top left: $B = -0.95$; Top right: $B = 0.7$. In the lower plot the domain corresponding to the Lorenz attractor in the Shimizu-Morioka model (the upper and right part of the red region of Fig.4) is transformed back to the (M_1, M_2) variables. The value of s is determined in such a way that $B = 0.7$.

An illustration of some of the attractors found for $B < 0$ with $|B|$ close to 1 is shown in Fig.2 right. The black points on it are successive iterates, under H^4_{B,M_1,M_2}, of some initial point. They are close to an unstable invariant curve. This curve becomes stable, for instance, changing M_2 from -0.925 to -0.900, having a rotation number close to $1/4$. The parameters of this strange attractor belong to the upper blue spot in Fig.6 left. The ones of the invariant curve are in the light blue domain on top of it.

We refrain from displaying strange attractors of different type and refer only to Figs.1 and 2. But it is interesting to compare the theoretical predictions with the numerical results. To this end it is possible to pass from the parameters (B, M_1, M_2) of the 3D Hénon map to the parameters (α, λ, s) of the Shimizu-Morioka model, including the scaling factor s, and vice versa. For a fixed value of s the value of β_1 is s^2 and, as (α, λ) must be finite, the values of β_2, β_3 are $O(s)$. Hence we expect the components of ε to be $O(s)$ and relatively close to the plane $\varepsilon_1 - \varepsilon_2 + \varepsilon_3 = 0$. For comparison purposes, instead of fixing s it is better to fix B. Hence, we have selected the open domain corresponding to the Lorenz attractor part of the "red" region of the Shimizu-Morioka system (see Fig.4). Then values of (M_1, M_2) and s have been determined according to the transformation of parameters. Using $B = 0.7$ the corresponding values of s range in $(0.14, 0.31)$. The result is displayed in the lower part of Fig.6. This domain should (except by some distortion, after all $s = 0.31$ is not so small) fit the "red" region of the 3D Hénon map. The agreement is quite good.

Thus, we can assume that a periodically perturbed Shimizu-Morioka system describes well the 3D Hénon map in this region of the parameter values. Therefore, a certain part of the blue region adjoining to the red one in the middle plot of Fig.6 can be related, on a qualitative level at least, to the region of the existence of a quasi-attractor in the Shimizu-Morioka model (this is the lower part of the red region in Fig.4(left)). Since an effective periodic force is applied, the windows corresponding to stable periodic orbits become windows of stable invariant closed curves. As we mentioned, the saddle-focus equilibria with two-dimensional unstable manifold play an important role in the quasi-attractor of the Shimizu-Morioka model, i.e. the chaotic trajectories may spend sufficiently large time in the neighborhood of these two points. The same may hold true for the 3D Hénon map in the corresponding region, thus providing a possible source for the numerically observed pair of positive Lyapunov exponents.

A direct computation of a Lyapunov diagram, similar to previous ones, for a periodically perturbed Shimizu-Morioka system, could be very interesting. Instead, we performed a similar experiment using a family of diffeomorphisms depending on an additional parameter, μ, which, in the limit $\mu \to 0$ behaves as the time μ map of (11). One possibility is to use the Euler step of (11) with step-size μ. This presents the problem that the map has non-constant Jacobian and for large values of the variables is no longer a diffeomorphism. As the Shimizu-Morioka system has constant negative divergence, it is always possible to construct an approximation to the time μ map with constant Jacobian, as follows:

$$\begin{pmatrix} X \\ Y \\ Z \end{pmatrix} \mapsto \begin{pmatrix} \bar{X} \\ \bar{Y} \\ \bar{Z} \end{pmatrix} = \begin{pmatrix} X + \mu\bar{Y} \\ Y + \mu(X(1-\bar{Z}) - \lambda Y) \\ Z + \mu(-\alpha Z + X^2) \end{pmatrix}. \tag{15}$$

This mimics the way in which the standard map is obtained as an approximation of the time μ map of a pendulum to keep it canonical. The map (15) has the Jacobian $J = (1-\mu\alpha)(1-\mu\lambda)$. If $\mu < \min\{1/\alpha, 1/\lambda\}$ one has a global diffeomorphism.

Using values like $\mu = 0.1$ or even $\mu = 0.3$ the results look very much like the ones displayed in Fig. 4 left for the flow. But it is possible to use a larger value of μ, so that the differences with the flow are increased. Figure 7 displays the results for $\mu = 0.8$. As done with the Shimizu-Morioka flow, the starting point has been taken in the unstable manifold of the origin. Up to 5×10^7 iterates have been used. A Lyapunov exponent Λ is considered as zero when $|\Lambda| < 4 \times 10^{-6}$. The same tolerance has been used to consider two Lyapunov exponents as similar. Even with this large μ and small tolerance, a region of strange attractors with one Lyapunov exponent very close to zero can be seen in the left part.

To conclude, we repeat that the theoretical results we described work in a sufficiently small neighborhood of the bifurcation point. It is a luck that the region of existence of Lorenz–like

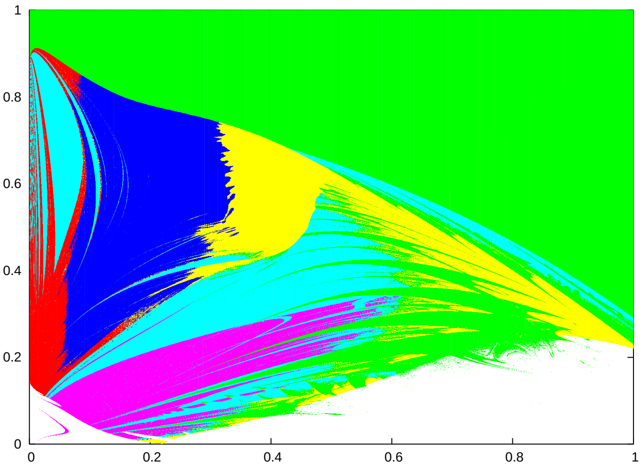

Figure 7: Lyapunov diagram for map (15) with $\mu = 0.8$. Plotted variables (α, λ). The color code is the same we used in Figs. 5 and 6.

pseudo-hyperbolic attractors in the 3D Hénon map extends sufficiently far in the parameter space, so it becomes visible. Still, a very large portion of the parameter space is occupied by regions corresponding to other types of dynamical behavior. What kinds of new structures show up in this map and in other three-dimensional maps, non-reducible to two-dimensional ones, this remains a question wide open for further studies.

Acknowledgements

The research of S.V.G. has been supported by grant UR.03.01.180, by RFBR grants No.04-01-00487 and 04-01-00483 (Russia), by CRDF-grant No. RU-M1-2583-MO-04 and by a NATO Scientific Committee fellowship-2004 Grant. The research of I.I.O. was supported by grants UR.03.01.180, RFBR No.04-01-00487 and No.04-01-00483, and "Leading Scientific Schools" No.838.2003.2 (Russia). The research of C.S. has been supported by grants DGICYT BFM2003-09504-C02-01 (Spain) and CIRIT 2001 SGR-70 (Catalonia). The cluster HIDRA of the UB Group of Dynamical Systems has been widely used. We are indebted to J. Timoneda for keeping it fully operative. D.T. thanks A.Gorodetsky and V.Kleptsyn for useful discussions.

References

Afraimovich, V.S., Bykov, V.V. & Shilnikov, L.P. [1977] "The origin and structure of the Lorenz attractor," *Sov. Phys., Dokl.* **22**, 253-255.

Afraimovich, V.S., Bykov, V.V. & Shilnikov, L.P. [1980] "On the existence of stable periodic orbits in the Lorenz model," *Russian Math. Surveys* **36**.

Afraimovich, V.S., Bykov, V.V. & Shilnikov, L.P. [1983] "On attracting structurally unstable limit sets of Lorenz attractor type," *Trans. Mosc. Math. Soc.* **44 (1982)**, 153–216.

Afraimovich, V.S. & Shilnikov, L.P. [1974] "On some global bifurcations connected with the disappearance of a fixed point of saddle-node type," *Sov. Math., Dokl.* **15**, 1761–1765.

Afraimovich, V.S. & Shilnikov, L.P. [1982] "Bifurcation of codimension 1, leading to the appearance of a countable set of tori," *Sov. Math., Dokl.* **25**, 101-105.

Afraimovich, V.S. & Shilnikov, L.P. [1983a] "Invariant two-dimensional tori, their breakdown and stochasticity," in *Methods of the qualitative theory of differential equations*, (Gorki), pp.3–26 [English translation in *Transl., Ser. 2, Am. Math. Soc.* **149 (1991)**, 201–212].

Afraimovich, V.S. & Shilnikov, L.P. [1983b] "Strange attractors and quasi-attractors," in *Nonlinear dynamics and turbulence*, *Interaction Mech. Math. Ser.* (Pitman) pp.1–34.

Arneodo, A., Coullet, P.H. & Spiegel, E.A. [1985a] "The dynamics of triple convection," *Geophys. Astrophys. Fluid Dyn.* **31**, 1–48.

Arneodo, A., Coullet, P.H., Spiegel, E.A. & Tresser, C. [1985b] "Asymptotic chaos." *Physica* **D 14**, 327–347.

Belykh, V.N. [1984] "Bifurcation of separatrices of a saddle point of the Lorentz system," *Differ. Equations* **20**, 1184-1191.

Bosch, M., Carcassés, J.P., Mira, C., Simó, C. & Tatjer, J.C. [1991a] "Crossroad area-spring area transition. (I) Parameter plane representation," *Bifurcation and Chaos* **1**, 183–196.

Bosch, M., Carcassés, J.P., Mira, C., Simó, C. & Tatjer, J.C. [1991b] "Crossroad area-spring area transition. (I) Foliated parametric representation," *Bifurcation and Chaos* **1**, 339–348.

Broer, H., Roussarie, R. & Simó, C. [1996] "Invariant circles in the Bogdanov-Takens bifurcation for diffeomorphisms," *Ergod. Th. & Dynam. Sys.* **16**, 1147–1172.

Broer, H., Simó, C. & Tatjer, J.C. [1998] "Towards global models near homoclinic tangencies of dissipative diffeomorphisms," *Nonlinearity* **11**, 667–770.

Broer, H., Simó, C. & Vitolo, R. [2005] "Chaos and quasi-periodicity in diffeomorphisms of the solid torus," in preparation.

Bykov, V.V. [1980] "Bifurcations of dynamical systems close to systems with a separatrix contour containing a saddle-focus," in *Methods of the qualitative theory of differential equations* (Gorky) pp.44–72.

Bykov, V.V. [1993] "The bifurcations of separatrix contours and chaos," *Physica* **D 62**, 290-299.

Bykov, V.V. & Shilnikov, A.L. [1989] "On the boundaries of the domain of existence of the Lorenz attractor," in *Methods of qualitative theory and bifurcation theory* (Gorky) pp.151-159 [English translation in *Selecta Math. Sov.* **11 (1992)**, 375-382].

Fenichel, N. [1971] "Persistence and smoothness of invariant manifolds for flows," *Indiana Univ. Math. J.* **21**, 193–226.

Gonchenko, S.V., Turaev, D.V. & Shilnikov, L.P. [1993] "Dynamical phenomena in multidimensional systems with a structurally unstable homoclinic Poincaré curve," *Russian Acad. Sci., Dokl., Math.* **47**(3), 410-415.

Gonchenko, S.V., Turaev, D.V. & Shilnikov, L.P. [2003] "On dynamical properties of diffeomorphisms with homoclinic tangencies," *Contemp. Math. and Appl.* **7**, 92-118 [English version: WIAS Preprint No.795 (2002)]

Gonchenko, S.V. & Ovsyannikov, I.I. [2005] "Three-dimensional Hénon map in homoclinic bifurcations," in preparation.

Gorodetskij, A.S. & Ilyashenko, Yu. S. [1999] "Some new robust properties of invariant sets and attractors of dynamical systems," *Funct. Anal. Appl.* **33**(2), 95–105.

Gorodetskij, A.S. & Ilyashenko, Yu. S. [2000] "Some properties of skew products over a horseshoe and a solenoid," *Proc. Steklov Inst. Math.* **4**, 90–112.

Gorodetskij, A., Ilyashenko, Yu., Kleptsyn, V., Nalsky, M. [2005] "Non-removable zero Lyapunov exponents," *Funct. Anal. Appl.* **39**(1).

Guckenheimer, J. [1976] "A strange, strange attractor," in *The Hopf bifurcation and its application*, eds. Marsden, J.E. & McCracen, M. (Springer-Verlag) pp.368-381.

Guckenheimer, J. & Williams, R.F. [1979] "Structural stability of Lorenz attractors," *Publ. Math. IHES* **50**, 59–71.

Lorenz, E. [1963] "Deterministic non-periodic flow," *J. Atmos. Sci.* **20**, 130–141.

Neishtadt, A. [1984] "The separation of motions in systems with rapidly rotating phase," *J. Appl. Math. Mech.* **48**, 133–139.

Ovsyannikov, I.M. & Shilnikov, L.P. [1987] "On systems with a saddle-focus homoclinic curve," *Math. USSR, Sb.* **58**, 557-574.

Ovsyannikov, I.M. & Shilnikov, L.P. [1992] "Systems with a homocline curve of a multidimensional saddle-focus, and spiral chaos," *Math. USSR, Sb.* **73**(2), 415-443.

Pisarevsky, V., Shilnikov, A. & Turaev, D. [1998] "Asymptotic normal forms for equilibria with a triplet of zero characteristic exponents in systems with symmetry," *Regular and Chaotic dynamics* **2**, 123–135.

Robinson, C. [1989] "Homoclinic bifurcation to a transitive attractor of Lorenz type." *Nonlinearity* **2**(4), 495-518.

Robinson, C. [1992] "Homoclinic bifurcation to a transitive attractor of Lorenz type. II." *SIAM J. Math. Anal.* **23**(5), 1255-1268.

Rychlik, M.R. [1990] "Lorenz attractors through Shilnikov-type bifurcation. I." *Ergodic Theory Dyn. Syst.* **10**(4), 793-821.

Sataev, E.A. [2005] "Nonautonomous perturbations of systems of Lorenz type do not lead to the emergence of stable periodic orbits," in preparation.

Shilnikov, A.L. [1986] "Bifurcation and chaos in the Morioka-Shimizu system," in *Methods of qualitative theory of differential equations* (Gorky) pp.180–193 [English translation in *Selecta Math. Soviet.* **10 (1991)**, 105–117].

Shilnikov, A.L. [1993] "On bifurcations of the Lorenz attractor in the Shimizu-Morioka model," *Physica* **D 62**, 338–346.

Shilnikov, A.L., Shilnikov, L.P. & Turaev, D.V. [1993] "Normal forms and Lorenz attractors," *Bifurcation and Chaos* **3**, 1123–1139.

Shilnikov, A.L., Shilnikov, L.P. & Turaev, D.V. [2004] "On some mathematical topics in classical synchronization," *Bifurcation and Chaos* **14**, 2143–2160.

Shilnikov, L.P. [1969] "On the question of the structure of the neighborhood of a homoclinic tube of an invariant torus," *Sov. Math., Dokl.* **9**, 624–628.

Shilnikov, L.P. [1981] "Bifurcation theory and quasi-hyperbolic attractors," *Russian Math. Surv.* **36**(4).

Shilnikov, L.P., Shilnikov, A.L., Turaev, D.V. & Chua, L.O. [1998] *Methods of Qualitative theory in nonlinear Dynamics. Part I.* (World Scientific).

Shilnikov, L.P., Shilnikov, A.L., Turaev, D.V. & Chua, L.O. [2001] *Methods of Qualitative theory in nonlinear Dynamics. Part II.* (World Scientific).

Shimizu, T. & Morioka, N. [1980] "On the bifurcation of a symmetric limit cycle to an asymmetric one in a simple model," *Phys. Lett.* **A76**, 201–204.

Tucker, W. [1999] "The Lorenz attractor exists," *C. R. Acad. Sci. Paris Sér. I Math.* **329**, 1197–1202.

Turaev, D.V. & Shilnikov, L.P. [1998] "An example of a wild strange attractor," *Sb. Math.* **189**(2), 137–160.

Turaev, D.V. & Shilnikov, L.P. [2005] "The Lorenz attractor under a small periodic forcing," in preparation.